Defect Studies of Ultra-Fine Grained Mg and Mg-Based Alloys Prepared by High Pressure Torsion

Jakub Čížek[1,a], Ivan Procházka[1,a], Bohumil Smola[1,a], Ivana Stulíková[1,a], Radomír Kužel[1,a], Zdeněk Matěj[1,a], Viktoriya Cherkaska[1,a], Rinat K. Ismalgaliev[2,b], Olya Kulyasova[2,b]

[1]Faculty of Mathematics and Physics, Charles University in Prague, V Holešovičkách 2, CZ-180 00 Praha 8, Czech Republic

[2]Institute of Physics of Advanced Materials, Ufa State Aviation Technical University, Ufa 450 000, Russia

[a]jcizek@mbox.troja.mff.cuni.cz

Keywords: Ultra fine grained metals, Mg alloys, High pressure torsion, Positron annihilation, Dislocations.

Abstract. Despite the favourable strength and thermal stability, a disadvantage of Mg-based alloys consists in a low ductility. Recently it has been demonstrated that ultra fine grained (UFG) metals with grain size around 100 nm can be produced by high pressure torsion (HPT). A number of UFG metals exhibit favourable mechanical properties consisting in a combination of a very high strength and a significant ductility. For this reason, it is highly interesting to examine microstructure and physical properties of UFG Mg-based light alloys. Following this purpose, microstructure investigations and defect studies of UFG Mg and selected UFG Mg-based alloys prepared by HPT were performed in the present work using positron annihilation spectroscopy (PAS) combined with X-ray diffraction (XRD), microhardness measurements, and direct observations of microstructure by TEM.

Positrons are trapped at dislocations in Mg and Mg-alloys deformed by HPT. In some cases number of dislocations increases with the radial distance r from the center to the margin of the sample most probably due to an increase of strain with r. No microvoids (small vacancy clusters) were detected. Mg-alloys deformed by HPT exhibit homogeneous UFG structure with grain size around 100 nm and high dislocations density except Mg-15%Gd alloy, where UFG structure was not formed. On the other hand, pure Mg deformed by HPT exhibits a binomial type of structure which consists of "deformed regions" with UFG structure and a high dislocation density and dislocation-free "recovered regions" with large grains. It indicates a dynamic recovery of microstructure during HPT processing.

Introduction

Lightweight Mg-based alloys enable to increase the effectiveness in automotive and air industries and in structural applications, which leads to a lower consumption of the fossil fuels and other energetic sources. However, the applicability of magnesium alloys is limited due to their low melting temperature T_m. A failure of the construction units can happen at temperatures higher than 0.4-0.5 T_m, i.e. 100-200°C. There is a big effort in materials science to extend the applicability of Mg-alloys to higher temperatures. The particularly promising way is use of rare earth alloying elements [1]. For example Mg-Gd system represents a promising novel hardenable material with high creep resistance even at elevated temperatures [2]. Despite the favourable strength and thermal stability, a disadvantage of Mg-based alloys with rear earth elements consists in a low ductility, which is not sufficient for industrial applications. Thus, attempts to enhance ductility of these alloys are highly desirable. Grain refinement is a well-known method how to increase ductility of metallic

materials. Recently it has been demonstrated that ultra fine grained (UFG) metals with grain size around 100 nm can be produced by high pressure torsion (HPT) [3]. A number of UFG metals exhibit favourable mechanical properties consisting in a combination of very high strength and a significant ductility. For this reason, it is highly interesting to examine microstructure and physical properties of UFG Mg-based light alloys. Following this purpose, microstructure investigations and defect studies of pure UFG Mg and selected perspective UFG Mg-based alloys were performed in the present work.

Experimental Details

The specimens of Mg (technical purity), Mg-10%Gd, Mg-15%Gd and Mg-4%Tb-2%Nd alloys were studied. The composition is given in the weight percents. We chose Mg-Gd binary system and Mg-Tb-Nd ternary alloy because of their promising mechanical properties and thermal stability [2]. The alloys were prepared from the technical purity Mg by squeeze casting. The as-cast material was subjected to homogenization annealing for 6 h at 500°C and 525 °C for Mg-Gd and Mg-Tb-Nd alloy respectively. The homogenization was finished by rapid quenching in water of room temperature. In addition, a well annealed high purity Mg (99.95 %) was used as a reference specimen. The UFG samples were prepared from the coarse grained initial materials by HPT at room temperature up to the true logarithmic strain $\varepsilon = 7$ under high pressure of 6 GPa [3]. The HPT deformed samples were disk shaped with diameter 12 mm and thickness 0.3 mm.

A fast-fast positron lifetime (PL) spectrometer similar to that described in [4] with timing resolution 160 ps (FWHM ^{22}Na) at the coincidence counts rate 120 s^{-1} was employed in the present work. A ^{22}Na positron source with activity 1.5 MBq sealed on 2 μm thick mylar foil was used. Decomposition of PL spectra into exponential components was performed using a maximum likelihood procedure [5]. The PL measurements were accompanied by theoretical calculations of positron lifetimes using the atomic superposition method (ATSUP) [6]. TEM observations were performed on the JEOL 2000 FX electron microscope operating at 200 kV. XRD studies were carried out with the aid of XRD7 and HZG4(Seifert-FPM) powder diffractometers using Cu K_α radiation. The microhardness Hv was measured by the Vickers method with a load of 100 g applied for 10 s using the LECO M-400-A hardness tester.

Results and Discussion

Coarse-grained materials. PL spectrum of the as-cast coarse-grained Mg specimen consists of two components listed in Table 1. The shorter component with lifetime τ_1 can be attribute to free positrons, while the longer one with lifetime $\tau_2 = 256$ ps comes from positrons trapped at defects. The lifetime τ_2 lies between the Mg bulk lifetime $\tau_B = 227$ ps [7] and the calculated lifetime of positrons trapped in Mg-monovacancy $\tau_v = 297$ ps. It is typical for dislocations. Dislocation density $\rho \approx 5\times10^{12}$ m^{-2} and the mean grain size of about 10 μm were estimated by TEM in this specimen. Thus, we conclude that positrons are trapped at dislocations introduced into the as-cast Mg during casting and shaping. In order to check experimentally this interpretation, a technical purity Mg sample was cold rolled to thickness reduction $\varepsilon = 40\%$. PL results for the cold rolled sample are given in Table 1. One can see that the second component in PL spectrum of the cold rolled sample exhibits indeed virtually the same lifetime τ_2 (see Table 1) as the as-cast Mg, but significantly higher intensity I_2 due to higher dislocation density. Hence, we can conclude that the lifetime of 256 ps corresponds to positrons trapped at Mg dislocations. Annealing of the as-cast Mg at 280°C for 30 min leads to a complete recovery of dislocations reflected also by a remarkable decrease of microhardness Hv (see the last column of Table 1). The annealed sample exhibits a single component PL spectrum with lifetime which agrees reasonably with the Mg bulk lifetime τ_B. It

indicates that dislocations were annealed out and virtually all positrons annihilate from the free state.

Table 1. Lifetimes and corresponding relative intensities of the exponential components resolved in PL spectra (except of the source contribution). The PL results for HPT deformed materials correspond to the center of the sample. Microhardness values Hv are shown in the last column. Hv values in center and at the margin of the sample are given in case of HPT deformed Mg and Mg-10%Gd which exhibit an increase of Hv with the radial distance from center of the specimen. The errors (one standard deviations) are given in parentheses.

Sample	τ_1 (ps)	I_1 (%)	τ_2 (ps)	I_2 (%)	Hv (MPa)
Mg as-received	204(4)	63(1)	256(1)	37(1)	440(40)
Mg annealed 280°C/30 min	225.3(4)	100	-	-	330(20)
Mg cold rolled	160(10)	14(4)	257(2)	86(4)	
Mg-10%Gd homogenized	220(4)	90.9(6)	301(9)	9.1(7)	680(30)
Mg-15%Gd homogenized	224.8(4)	100	-	-	890(50)
Mg-4%Gd-2%Nd homogenized	220(1)	91(1)	280(10)	9(1)	450(30)
HPT Mg	188(5)	39(1)	257(3)	61(1)	570(30)-620(30)
HPT Mg-10%Gd	210(3)	34(2)	256(3)	66(2)	1670(40)-2330(40)
HPT Mg-15%Gd	221(2)	71(2)	256(3)	29(5)	1310(60)
HPT Mg-4%Tb-2%Nd	180(2)	14.9(4)	254(2)	85.1(4)	1090(10)

PL spectrum of the homogenized Mg-10%Gd alloy is well fitted by two components given in Table 1. The first component with the lifetime $\tau_1 < \tau_B$ and dominant intensity can be attributed to free positrons, while the second one with the lifetime τ_2 comes from positrons trapped at defects. TEM investigations of this sample revealed large coarse grains and a low dislocation density below $\approx 10^{12}$ m^{-2}, which approaches the lower sensitivity limit of PL spectroscopy [8]. Therefore, positrons trapped at dislocations cannot represent a noticeable contribution to PL spectrum. The component represents rather a contribution of positrons trapped in quenched-in excess vacancies "frozen" in the sample due to the rapid quenching. This interpretation is supported by the lifetime τ_2 $\approx$ 300 ps, which agrees well with the calculated lifetime τ_V of positrons trapped in Mg-monovacancy. As free monovacancies are not stable in Mg at room temperature [9], the observed defects represent vacancies bound to Gd atoms. It was proved by our coincidence Doppler broadening studies [10]. Positron trapping in the quenched-in vacancies bound to alloying elements, i.e. Tb or Nd, were detected also in homogenized Mg-4%Tb-2%Nd alloy, see Table 1 - the component with lifetime τ_2. Surprisingly no quenched-in vacancies could be found in homogenized

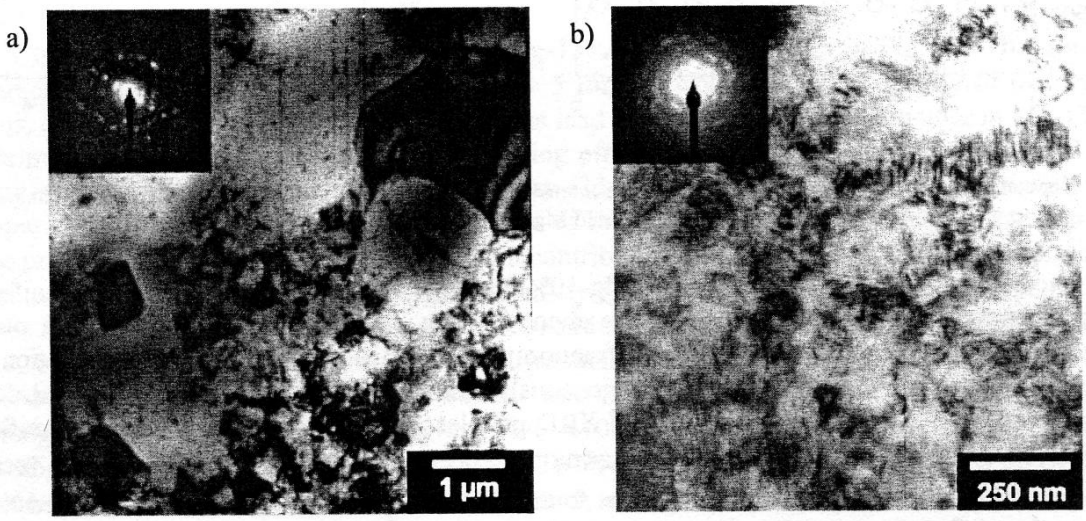

Fig.1: Bright-field TEM image of a) Mg b) Mg-10%Gd alloy deformed by HPT.

Mg-15%Gd alloy.

HPT deformed specimens. A representative TEM image of the HPT deformed Mg specimen is shown in Fig. 1a. Two different kinds of regions were observed: i) "deformed regions" with UFG grains (100-300 nm) and a high dislocation density, and ii) "recovered regions" with substantially larger grains (≈ 1 μm) and almost free of dislocations. The presence of the "recovered regions" indicates some kind of dynamic recovery of microstructure during the HPT processing. The XRD back-reflection pattern of HPT deformed Mg is a superposition of isolated spots and continuous diffraction rings, which testifies co-existence of the two kinds of regions [7,10]. The sample shows a texture of (001) type. No significant broadening of XRD profiles was detected so that dislocation density should be less than about $1\times10^{13}m^{-2}$. However, a major contribution to the diffraction peaks comes from the "recovered regions" so that the "deformed regions" cannot be well characterized by XRD. The PL spectrum of the HPT deformed Mg consists of the free positron component and a contribution of positrons trapped at dislocations. The lifetime τ_2 of the latter component agrees well with that found in cold rolled Mg for positrons trapped at dislocations. Hence, we can conclude that positrons are trapped at dislocations inside the "deformed regions". One can see in Table 1 that HPT deformed Mg exhibits remarkably higher value of microhardness Hv compared to the as-cast Mg. A slight increase of Hv with the radial distance r from center of the specimen was observed in HPT deformed Mg, see Fig. 2a. The Hv values for center of the sample and the margin are given in the last column of Table 1. To explain the behavior of microhardness we performed PL measurements at various distances r from center of the specimen. The dependence of relative intensity I_2 of the dislocation component on r is shown in Fig. 2b. Clearly I_2 exhibits a pronounced increase with r indicating an increase of dislocation density from center of the specimen to the margin.

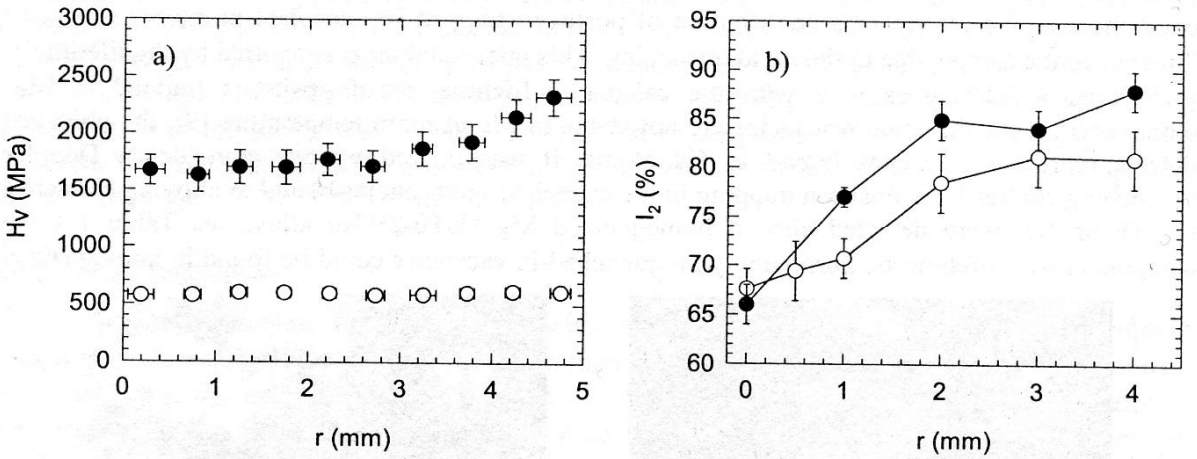

Fig.2: Dependence of a) microhardness Hv b) relative intensity I_2 of the PL defect component on the radial distance r from the center of sample. Full circles – HPT deformed Mg-10wt.%Gd, open circles – HPT deformed Mg.

A typical TEM image of HPT deformed Mg-10%Gd alloy is shown in Fig. 1b. It shows uniform UFG microstructure with the mean grain size about 100 nm, i.e. no dynamic recovery took place during the HPT processing. The electron diffraction pattern testifies high-angle missorientation of neighboring grains. A high density of homogeneously distributed dislocations was observed. It is reflected also by a significant broadening of XRD profiles. A lower broadening of (00l) profiles with respect to other peaks indicates a dominating presence of ⟨a⟩ dislocations with Burgers vector $\vec{b} = 1/3.a.[2\bar{1}\bar{1}0]$. A weak (001) texture was found. The PL spectrum of the HPT deformed Mg-10%Gd alloy consists of two components, see Table 1. The first component with the lifetime τ_1 comes from free positrons. The lifetime τ_2 of the second component corresponds well with that of positrons trapped at Mg-dislocations. One can see in Table 1 that I_2 values for HPT deformed Mg-

10%Gd and HPT deformed pure Mg are comparable despite the fact that the latter exhibits remarkably lower dislocation density. This surprising effect might be explained by a smaller specific positron trapping rate for dislocations in Mg-10%Gd alloy, where mainly partial dislocations are present due to a lower stacking fault energy, for details see [10]. However, this problem remains still open and requires additional investigations. Intensity I_2 of the dislocation component as a function of the radial distance r from center of the sample is plotted in Fig. 2b. Behavior of I_2 with r indicates that dislocation density increases from center of the specimen towards margin, see [7] for details. Increase of dislocation density with r is reflected also by significant increase of microhardness, see Fig. 2a.

a) b)

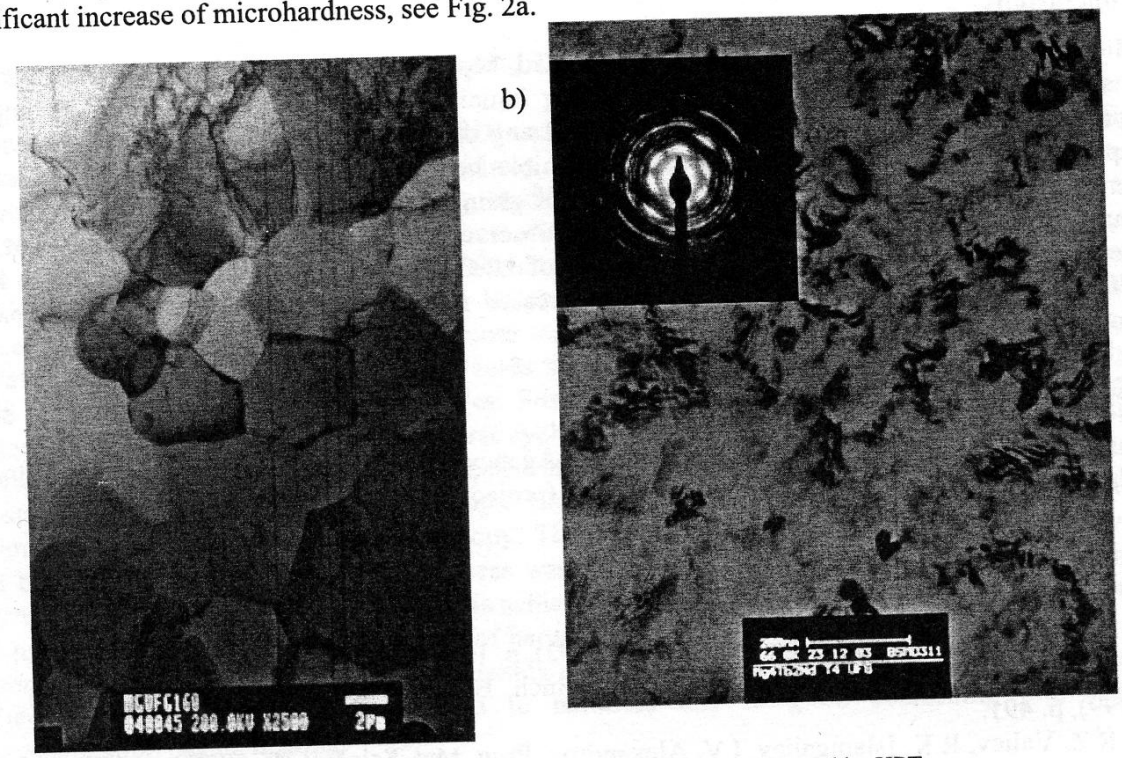

Fig.3: Bright-field TEM image of a) Mg-15%Gd b) Mg-4%Tb-2%Nd alloys deformed by HPT.

A typical TEM image of HPT deformed Mg-15%Gd alloy is shown in Fig. 3a. This sample is characterized by significantly larger grains ($\approx$ 5 μm) as well as a lower density of dislocations. Thus, contrary to Mg-10%Gd alloy, HPT did not lead to formation of UFG structure in Mg-15%Gd. It is most probably due to the solution hardening effect which makes deformation of Mg-15%Gd alloy more difficult. These results show that Gd content is a very important parameter in preparation of UFG Mg-Gd alloys. PL spectrum of HPT deformed Mg-15%Gd alloy consists of the free positron component with lifetime τ_1 and a contribution of positrons trapped at dislocations with lifetime τ_2 = 256 ps, see Table 1. Relative intensity I_2 of the dislocation component is more than 2 times lower compared to HPT deformed Mg-10%Gd sample due to a lower density of dislocations.

A bright-field TEM image and electron diffraction pattern for HPT deformed Mg-4%Tb-2%Nd is shown in Fig. 3b. It exhibits very similar microstructure as HPT deformed Mg-10%Gd, i.e. homogeneous UFG structure with grain size ≈100 nm and high density of homogeneously distributed dislocations. HPT deformed Mg-4%Tb-2%Nd exhibits two-component PL spectrum, see Table 1. The shorter component with lifetime τ_1 comes from free positrons while the longer component with lifetime τ_2 represents a contribution of positrons trapped at dislocations. High dislocation density is testified by relative intensity I_2 of the dislocation component, which is the highest one among all the studied samples.

A significant increase of microhardness Hv in HPT deformed specimens compared to corresponding coarse-grained materials was observed in all the samples studied, see the last column of Table 1. HPT deformed Mg-10%Gd alloy exhibits the highest Hv values as well as the highest increase of Hv caused by HPT. It amounts 143 % in center of the sample and 243 % at the margin. It should be mentioned that increase of Hv with the radial distance r from center of the specimen was observed in HPT deformed Mg and Mg-10%Gd. On the other hand, Hv does not vary with r in HPT deformed Mg-15%Gd and Mg-4%Tb-2%Nd.

Conclusions

Microstructure of HPT deformed Mg, Mg-10%Gd, Mg-15%Gd, and Mg-4%Tb-2%Nd alloys was characterized and compared with corresponding initial coarse grained materials. An incomplete dynamic recovery took place during HPT processing of Mg sample which resulted in a binomial type of structure. The HPT made Mg-10%Gd exhibits homogeneous UFG microstructure with high density of uniformly distributed dislocations and grain size about 100 nm. No microvoids were found. Very similar kind of microstructure was observed in HPT deformed Mg-4%Tb-2%Nd. On the other hand, HPT did not led to formation of UFG structure in Mg-15%Gd alloy. All HPT deformed specimens exhibit a significantly increased microhardness compared to initial coarse-grained materials.

Acknowledgement

This work was supported by The Czech Grant Agency (contract 106/01/D049), The Ministry of Education, Youth and Sports of Czech Republics (project 1K03025), and by DFG.

References

[1] B.L. Mordike, Mat. Sci. Eng. A Vol. 324 (2002), p. 103.
[2] P. Vostrý, B. Smola, I. Stulíková, F. von Buch, B.L. Mordike, phys. stat. sol. (a) Vol. 175 (1999), p. 491.
[3] R.Z. Valiev, R.K. Islamgaliev, I.V. Alexandrov, Prog. Mat. Sci. Vol. 45 (2000), p. 103.
[4] F. Bečvář, J. Čížek, L. Lešťak, I. Novotný, I. Procházka, F. Šebesta, Nucl. Instr. Meth. A Vol. 443 (2000), p. 557.
[5] I. Procházka, I. Novotný, F. Bečvář, Mat. Sci. Forum Vol. 225-257 (1997), p. 772.
[6] M.J. Puska, R.N. Nieminen, J. Phys. F: Met. Phys. Vol. 13 (1983), p. 333.
[7] J. Čížek, I. Procházka, B. Smola, I. Stulíková, R. Kužel, Z. Matěj, V. Cherkaska, R.K. Islamgaliev, O. Kulyasova, Mat. Sci. Forum (2004) accepted for publication.
[8] P. Hautojärvi, C. Corbel in: *Proceedings of the International School of Physics "Enrico Fermi", Course CXXV*, Ed. A. Dupasquier, A.P. Mills, IOS Press, Varena 1995, p. 491.
[9] M. Fahnle, B. Meyer, J. Mayer, J.S. Oehrens, G. Bester, in: *Diffusion Mechanisms in Crystalline Materials,* Ed. Y. Mishin, MRS Symposia Proceedings No. 527, p. 23.
[10] J. Čížek, I. Procházka, B. Smola, I. Stulíková, R. Kužel, Z. Matěj, V. Cherkaska, R.K. Islamgaliev, O. Kulyasova, Acta Physica Polonica A (2004) submitted for publication.